

Formulation and Biological Evaluation of Curcumin-Loaded Liposomes and PLA Nanoparticles against Oxidative Injury in NRK-52E Cells

Kauther I. Layas^{1*}, Mohammed I. Abdulkarim²

¹Pharmacy department, Oil clinic, Tripoli, Libya

²Research & Development, Libyan Foreign Investment Company, Tripoli, Libya

Corresponding email. k.layas@oilclinic.ly

Abstract

Curcumin is a natural polyphenol with antioxidant and anti-inflammatory properties. However, its low aqueous solubility and poor oral bioavailability limit clinical translation. In this study, curcumin was encapsulated into liposomes and PLA nanoparticles to evaluate formulation characteristics and biological effects in renal NRK-52E cells. Liposomal stability was assessed over 10 days using particle size distribution and zeta potential measurements, and physical observations indicated aggregation/precipitation from day 3 onward, with discontinuation after day 10 due to visible fungal-like growth. For PLA nanoparticles, thermal analysis suggested retention of the PLA glass transition. Drug loading was quantified by encapsulation efficiency (EE) and drug loading efficiency (LE). Curcumin-loaded formulations were evaluated for cytotoxicity and oxidative-stress modulation using MTT and LDH assays after exposure to either curcumin in different forms or the oxidative agent paraquat (PQ). At low curcumin concentrations, minimal changes were observed in viability and membrane integrity, whereas higher doses reduced cell viability and increased LDH release, with effects varying by formulation. During PQ challenge experiments, curcumin encapsulated in liposomes or PLA nanoparticles produced inconsistent outcomes and did not uniformly ameliorate oxidative injury. Overall, the results highlight formulation-dependent biological effects and underscore the need for assay-interference controls when evaluating curcumin in LDH-based readouts.

Keywords. curcumin, liposomes, PLA nanoparticles, paraquat, NRK-52E, LDH, MTT.

Introduction

Curcumin is a polyphenolic compound derived mainly from turmeric (*Curcuma longa*). Chemically, it is 1,7-bis(4-hydroxy-3-methoxyphenyl)-1,6-heptadiene-3,5-dione (Stanic 2017). Curcumin is a yellow, lipophilic solid with a reported logP of approximately 3.0. It is practically insoluble in water but soluble in polar organic solvents such as DMSO, methanol, ethanol, acetonitrile, chloroform, and ethyl acetate. In hydrocarbon solvents, solubility is limited, which contributes to formulation challenges (Priyadarsini 2014). Preclinical studies have suggested potential protective effects of curcumin in acute kidney injury (AKI) models in rats, including mechanisms related to antioxidant defense and modulation of inflammatory pathways. Reported antioxidant mechanisms include scavenging reactive oxygen species (ROS) and reactive nitrogen species (RNS), upregulation of heme oxygenase and glutathione transferase, and downregulation of xanthine oxidase. In addition, curcumin has been reported to inhibit protein kinases and downregulate pro-inflammatory proteins, cytokines, growth factors, and transcription factors (Nabavi *et al.*, 2011; Hismiogullari *et al.*, 2015; Fan *et al.*, 2017; Ugar *et al.*, 2014; Najafi *et al.*, 2015; Mercantepe *et al.*, 2018; Tapia *et al.*, 2014; Liu *et al.*, 2017; Topcu-Tarlacalisir *et al.*, 2016; Kaur *et al.*, 2016).

Despite promising *in vitro* and *in vivo* evidence, clinical trials in humans have not demonstrated clear benefits. A key limitation is curcumin's low oral bioavailability, which can be attributed to poor solubility, intestinal metabolism, and first-pass degradation (Garg *et al.*, 2018). To improve bioavailability and biological performance, formulation strategies have been explored, including incorporation into liposomes (Rogers *et al.*, 2011) and encapsulation into nanoparticles (Chen *et al.*, 2017). In this work, curcumin was encapsulated into liposomes and PLA nanoparticles and characterized for physicochemical properties, stability, and activity in NRK-52E cells using paraquat (PQ)-challenged experiments.

Material and Methods

Preparation of curcumin-loaded PLA nanoparticles

The method involved in the preparation of PLA nanoparticles in this study was DESD (Buhecha *et al.*, 2019), which was adopted and modified as required. An emulsion was made by mixing 10 mL 2% PVA solution with 200mg PLA

dissolved in 10ml DCM and 10ml acetone. This emulsion was then transferred into an excess amount of water (100 mL) with continuous homogenizing for 15 min at 15000 rpm. Any organic solvent was then removed overnight. After centrifugation, Pellets (containing nanoparticles) were frozen and freeze dried and stored in a fridge [Figure 1].

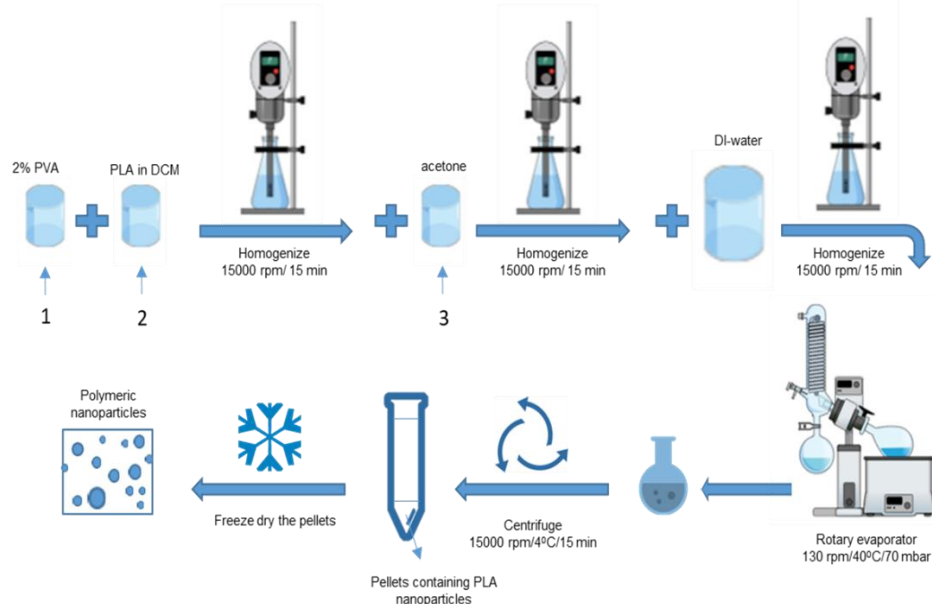


Figure 1. Formulation of PLA nanoparticles

Preparation of curcumin-loaded liposomes

The method used for the preparation of liposomes was based on the hydration of lipid film to prepare large multilamellar vesicles, followed by membrane extrusion to form small unilamellar vesicles (Dichello *et al.*, 2017). 5ml DPPC solution of curcumin was evaporated using a rotary evaporator to form a uniform lipid layer. Subsequently, 4ml water was added to this film while shaking vigorously and sonicating for 10 min. For particle size reduction of the liposomes, an Avanti mini-extruder with a 200 nm pore size polycarbonate membrane and glass air-tight syringes was used [Figure 2].

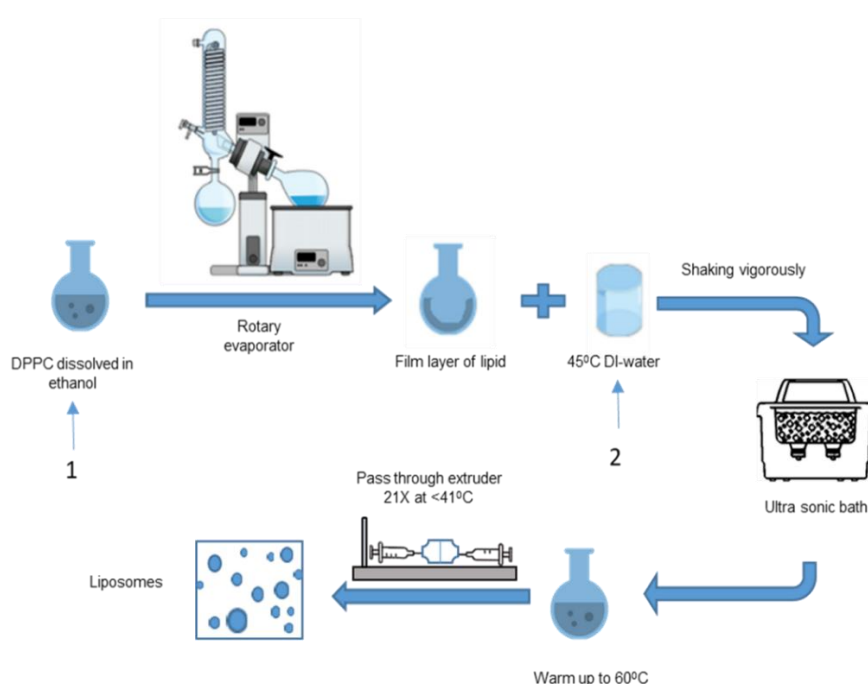


Figure 2. formulation of liposomes

Physical characterization of liposomes and nanoparticles

The produced PLA nanoparticles and liposomes were characterized for their particle size, zeta-potential, surface morphology, stability, drug loading, thermal properties, and antioxidant activity. Liposomes were only characterized for their morphology using LM. PLA nanoparticles were examined using ZEISS Sigma Field Emission Gun SEM with an Everhart Thornley-Secondary Electron detector. Thermal analysis of the PLA nanoparticles was studied using a differential scanning calorimeter (DSC). Fourier transform-infrared spectroscopy (FT-IR) was used to detect if any excess drug had adhered to the particles or if there were any interactions between the drug and polymer. Three curcumin-loaded liposomal samples were tested for stability evaluation over 10 days. Particle size, polydispersity index (Pdl), and zeta potential were measured on days 1, 2, 3, 4, 8, and 10.

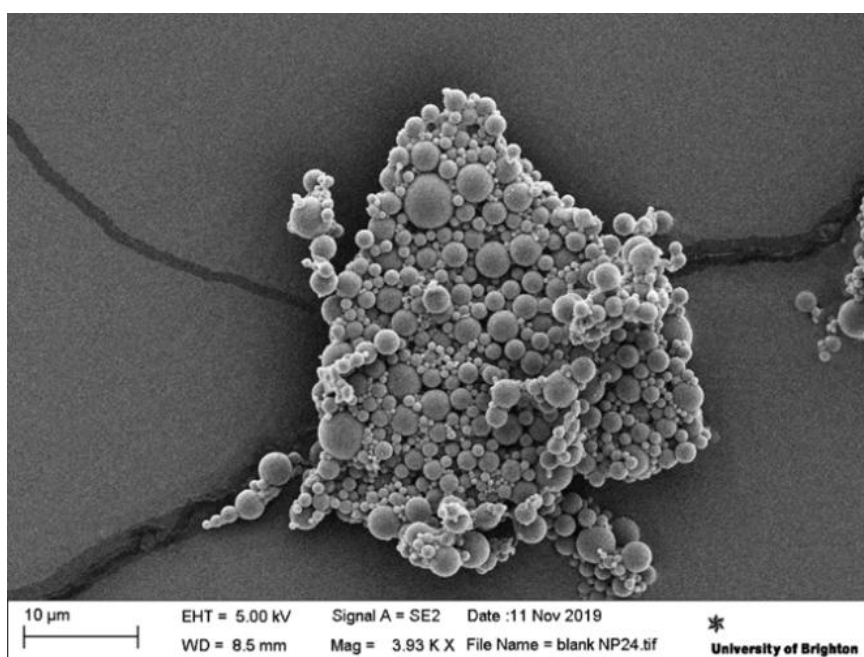


Figure 3. SEM image of blank PLA nanoparticles

Drug loading and encapsulation efficiency

High-performance liquid chromatography (HPLC) was used to calculate the concentration of curcumin in all samples after extraction and to measure the amount of drug entering cells when performing *in vivo* studies. Agilent 1220 series, attached to Clarity-Chromatography SW, DataApex software, Agilent 1220 pump system, manual injector with a 20 μ L injection loop, and an Agilent 1220 UV-visible detector. A 5 μ m Fortis C18, 150 * 4.6 mm column was used with 0.1% v/vTFA: acetonitrile (50:50) as mobile phase, at a flow rate of 1.5 ml/min at 25°C with a detector wavelength of 420 nm. Standard concentrations over the range of 0.1–20 μ g/ml were prepared. %LE was calculated as described by Jadhav *et al.*, 2007.

Cytotoxicity and internalization in NRK-52E cells

NRK-52E cells were used to evaluate internalization and toxicity of antioxidant-loaded nanoparticles in comparison to the free antioxidant solution. After 24 h of exposure, internalization was calculated from the recovered concentration. NRK-52E cells were obtained at passage 15 and used within passage 16-26. The MTT assay was used to assess cell viability in this study (Mossmann 1983, Abe & Matsuki 2000). On the other hand, the LDH assay, described by Abe & Matsuki (2000, was used to test the integrity of the cell membrane (cell death). Furthermore, oxidative-stress responses were assessed in NRK-52E cells using MTT and LDH assays, using paraquat (PQ)-challenged experiments. PQ was used to bring injury to NRK-52E cells *in vitro*, to mimic the oxidant damage induced on renal tubular epithelial cells during AKI (Elisha-Lambert 2017). Cells were pre-incubated for 24 h with curcumin-loaded liposomes, curcumin-loaded PLA

nanoparticles, or free curcumin solution, then challenged with increasing PQ concentrations (0–1 mM). Formulation concentrations were selected based on actual curcumin loading and theoretical concentrations [Table 1]. Statistical analysis was performed using ordinary two-way ANOVA and Bonferroni *post hoc* comparisons.

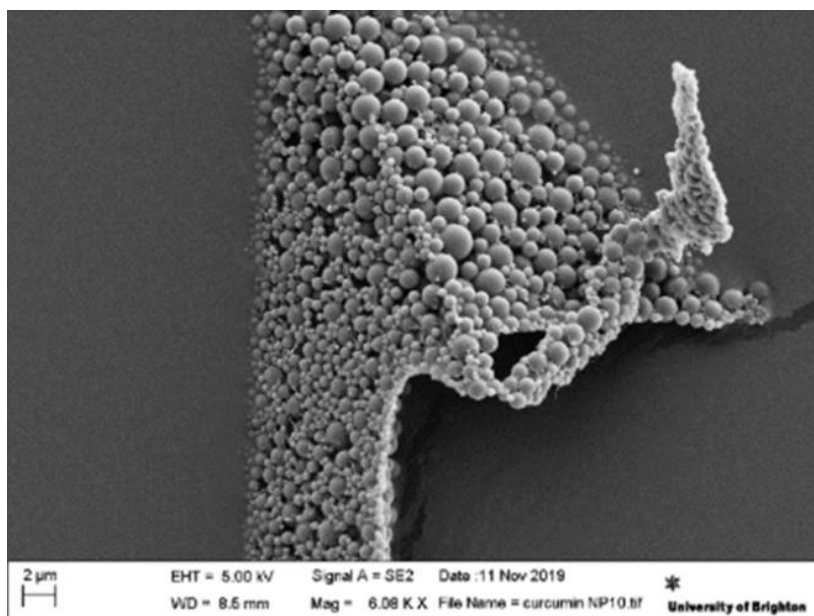


Figure 4. SEM image of curcumin loaded PLA nanoparticles

Table 1. The concentration of curcumin in each sample and its given code

| Drug | Form | Theoretical conc (μg/mL) | %LE | Actual conc (μg/mL) | code |
|----------|-------------------|--------------------------|--------|---------------------|------|
| Curcumin | liposomes | 6.25 | 52.90% | 3.31 | CL-1 |
| Curcumin | liposomes | 62.5 | 52.90% | 33.06 | CL-2 |
| Curcumin | PLA nanoparticles | 6.25 | 52.35% | 3.27 | CP-1 |
| Curcumin | PLA nanoparticles | 62.5 | 52.35% | 32.72 | CP-2 |
| Curcumin | solution | 6.25 | NA | 6.25 | CS-1 |
| Curcumin | solution | 62.5 | NA | 62.5 | CS-2 |

Results

Physical characterization of liposomes and nanoparticles

Liposomes have shown a smaller particle size ($210.4 \pm 60.2\text{nm}$) compared to PLA nanoparticles ($319.5 \pm 80.29\text{ nm}$). The PDI observed for liposomes (0.051) was less than that observed for PLA nanoparticles (0.206). Drug-loaded nanoparticles did not show a significant difference in size compared to blank nanoparticles. PLA nanoparticles showed a more negative zeta-potential on the surface of the particles ($-30.5 \pm 7.27\text{mV}$) compared to the liposomes ($-11.6 \pm 3.97\text{mV}$). Liposomal samples showed sizes before the extrusion step in the micron range and dropped to below 300 nm when extruded. SEM images for blank PLA nanoparticles and for PLA nanoparticles encapsulated with curcumin are shown below in figures 3,4. Overall, the images show that PLA nanoparticles are spherical in shape with a wide size distribution range. Thermal analysis of curcumin-loaded PLA nanoparticles demonstrated a glass transition temperature (T_g) at approximately $45.46\text{ }^\circ\text{C}$, and a small endothermic event was observed between 210 and $220\text{ }^\circ\text{C}$ [Figure 5]. FT-IR spectrum of free curcumin [Figure 6] revealed the presence of C-H vibration, C-O-C peak, C-O (enol) peak, aromatic C=C stretch, and O-H peak around 900 , 1030 , 1290 , 1500 , 3500 cm^{-1} , respectively. However, these characteristic peaks were not observed in the spectra produced from the curcumin-loaded PLA nanoparticles.

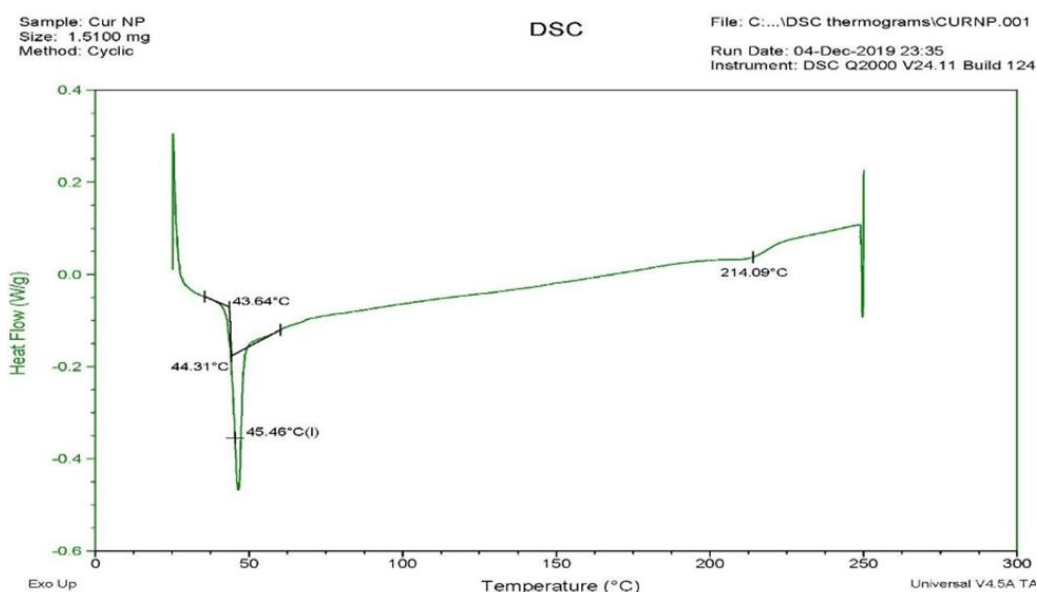


Figure 5. A thermogram for curcumin PLA nanoparticles

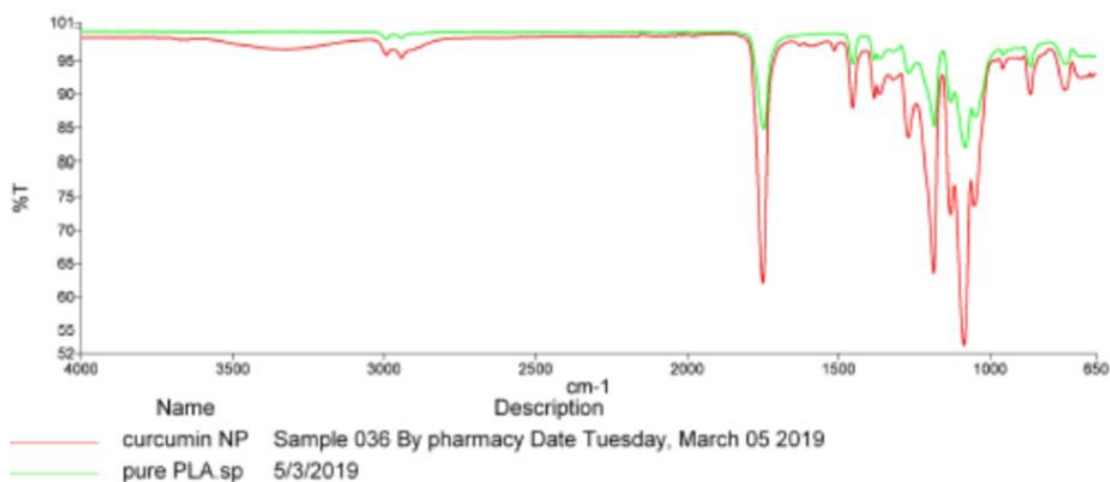


Figure 6. FT-IR spectrum for curcumin-loaded nanoparticles (in red) and PLA (in green)

Stability of curcumin-loaded liposomes

Results of the stability study are summarized in (Table 2) (mean \pm SD, $n=3$). On day 1, the mean particle size was 132.8 \pm 79.18nm. On day 2, the mean size increased to 147.4 \pm 91.77nm with no significant change reported. Notably, starting from day 3, the size distribution became bimodal, with a first peak in the approximate range of 105.3–189.1nm and a second peak corresponding to very large particles (approximately 4640–5224 nm). The volume fraction (%V) associated with the first peak decreased over time (100% on day 1 to 49.5% on day 3), while the %V of the second peak increased correspondingly (0% on day 1 to 50.5% on day 3). By day 10, the second peak dominated the distribution (%V = 95.2%), indicating progression toward aggregation or coalescence. PDI increased over the monitoring period, rising from 0.160 on day 1 to 0.227 on day 10, consistent with loss of size homogeneity. Zeta potential remained within an approximate range of -10.3 to -12.6mV, with no substantial day-to-day change observed. Physical observation supported the instrumental results. On days 1 and 2, samples appeared yellowish and transparent without visible precipitation. From day 3 onward, a yellow precipitate formed at the bottom of the tube and increased over time, consistent with curcumin release. By day 10, changes in color and viscosity were observed, and the stability study was discontinued due to fungal-like growth.

Drug loading and encapsulation efficiency

For curcumin-loaded PLA nanoparticles, drug loading efficiency (LE) was $52.35 \pm 22.65\%$ compared to encapsulation efficiency (EE): $73.8 \pm 1.22\%$. For liposomal formulations, on the other hand, the reported LE of curcumin was $52.90 \pm 11.11\%$

Table 2. Size distribution and zeta-potential of curcumin loaded liposomes from day one of preparation until day ten

| Day | Peak 1 (nm) | Peak 2 (nm) | PdI | Zeta-potential (mV) |
|-----|---------------------------|--------------------------|-------|---------------------|
| 1 | 132.8 ± 79.18 (100%) | - | 0.160 | -12.6 ± 3.92 |
| 2 | 147.4 ± 91.77 (100%) | - | 0.172 | -10.74 ± 3.65 |
| 3 | 153.9 ± 68.99 (49.5%) | 5063 ± 820.0 (50.5%) | 0.202 | -11.99 ± 3.06 |
| 4 | 164.2 ± 54.24 (39.3%) | 5224 ± 742.6 (60.7) | 0.219 | -11.7 ± 4.22 |
| 8 | 105.3 ± 50.54 (28.9%) | 4859 ± 116.0 (71.1%) | 0.212 | -10.3 ± 4.32 |
| 10 | 189.1 ± 95.0 (4.8%) | 4640 ± 142.9 (95.2%) | 0.227 | -11.5 ± 3.21 |

Cytotoxicity and internalization in NRK-52E cells

Liposomal samples showed higher %internalization for curcumin ($24.98 \pm 0.22\%$) compared to free curcumin ($4.22 \pm 0.02\%$) and curcumin-loaded PLA nanoparticle samples ($25.44 \pm 0.10\%$). No significant variation in either MTT formation or LDH release was detected using a low dose of all curcumin samples. As opposed to using high concentration, which showed a momentous effect on cells. For instance, using $26.12 \mu\text{g/mL}$ curcumin-loaded liposomes showed a reduction in cell viability up to $86.96 \pm 6.01\%$. This was consistent with the noted increase in LDH releases using the same concentration ($63.06 \pm 6.35\%$ increase in LDH release). However, there was a rather significant increase in LDH release observed ($21.15 \pm 3.20\%$ & $28.11 \pm 3.20\%$), even when using lower concentrations (6.53 & $13.06 \mu\text{g/mL}$). Moreover, using high doses of curcumin-loaded PLA nanoparticles (8.35 & $18.56 \mu\text{g/mL}$) showed a higher reduction in cell viability than liposomes, measured by MTT ($74.79 \pm 24.49\%$ & $72.83 \pm 22.58\%$, respectively). Mean \pm SD, N = 6, ** p < 0.01, *** p < 0.001 vs blank [0 $\mu\text{g/mL}$] [Figure 7].

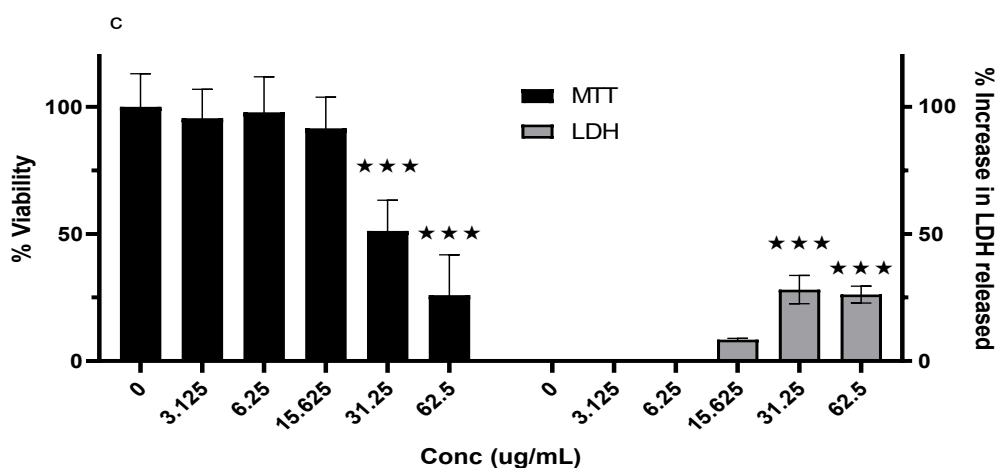


Figure 7. The effect of increased concentration of curcumin in three different forms on NRK-52E cells was measured using two different assays: MTT and LDH. a. curcumin-loaded liposomes. b. curcumin-loaded PLA nanoparticles. c. curcumin suspension

Although the SD were quite high, which may indicate loss of precision, the loss in cell viability was confirmed by the increase in LDH release using the same concentrations ($92.19 \pm 9.92\%$ & $92.19 \pm 9.34\%$; respectively). However, using high concentrations of curcumin solution also led to a significant reduction in cell viability ($51.22 \pm 12.03\%$ & $25.94 \pm 15.88\%$), which was confirmed by the increase in LDH release ($28.10 \pm 5.56\%$ & $26.16 \pm 3.32\%$) using the same

concentrations (31.25 & 62.5 $\mu\text{g}/\text{mL}$; respectively). However, these concentrations were much higher than the curcumin concentration in the PLA nanoparticles, also causing a significant reduction. It should be pointed out that using 15.63 $\mu\text{g}/\text{mL}$ curcumin in suspension showed only an insignificant reduction in cell viability ($91.60 \pm 12.21\%$), confirmed by an insignificant increase in LDH release ($8.38 \pm 0.56\%$), indicating that the PLA nanoparticle form of curcumin had a more harmful effect using comparable concentrations.

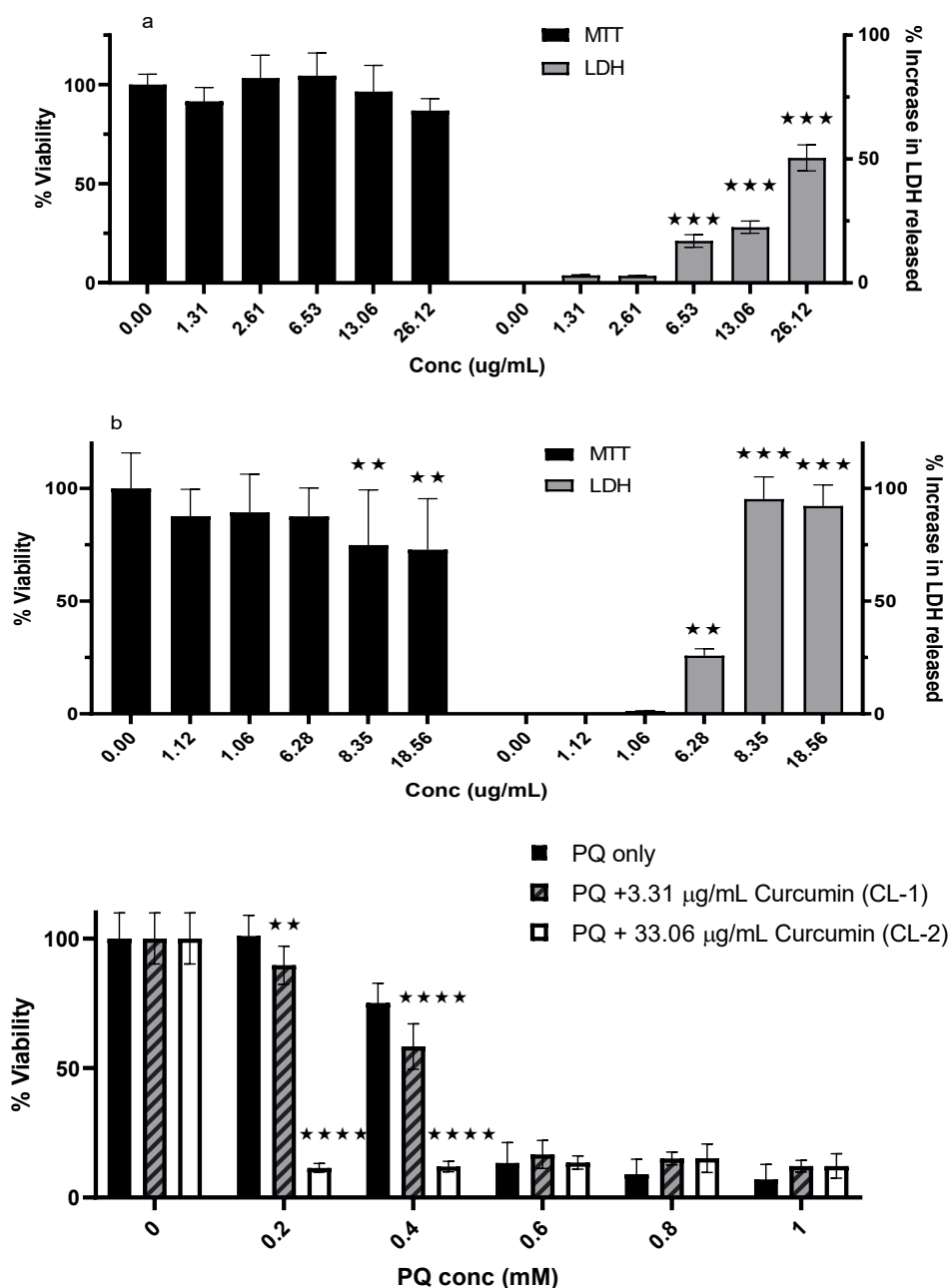


Figure 8. The effect of two different concentrations of curcumin-loaded liposomes plus PQ compared to PQ only on %viability of cells using the MTT assay

PQ challenge experiments (pre-incubation with curcumin formulations)

Results showed that curcumin-loaded liposomes further reduced the viability of the cells. The %viability using 0.2 mM PQ changed from $100.69 \pm 7.95\%$ to $89.66 \pm 7.34\%$ & $11.44 \pm 1.71\%$ when pre-incubating with CL-1 & CL-2, respectively.

Furthermore, the %viability using 0.4 mM PQ was dropped from $75.16 \pm 7.54\%$ to $58.3 \pm 8.73\%$ and $11.97 \pm 2.03\%$ when pre-incubating with the same concentrations, respectively. No significant change was observed using pre-incubation of either CL-1 or CL-2 after treatment with ≥ 0.6 mM PQ. Mean \pm SD, N = 6, $p < 0.0001$, $**p < 0.01$, $****p < 0.0001$ compared to PQ only [Figure 8]. This was generally consistent with the results from the LDH assay. The %increase in LDH after 0.4 mM PQ treatment ($56.03 \pm 8.39\%$) was additionally increased to $107.71 \pm 7.33\%$ & $100.44 \pm 3.41\%$ using pre-incubation with CL-1 & CL-2, respectively. The %increase in LDH test also amplified after treating with 0.2 mM PQ from $15.53 \pm 6.51\%$ to $111.34 \pm 5.88\%$ when pre-treating with CL-2. Nevertheless, a substantial reduction in the %LDH release was noticed when pre-incubating with CL-1 ($2.56 \pm 1.66\%$). No substantial protection was noticed using curcumin-loaded liposomes after treatment with ≥ 0.6 mM PQ, although there were small reductions in %increases in LDH release using both CL-1 & CL-2. Mean \pm SD, N = 6, $p < 0.0001$, $**p < 0.01$, $***p < 0.001$, $****p < 0.0001$ compared to PQ only [Figure 9].

Effect of pre-incubation with curcumin-loaded PLA nanoparticles

The use of curcumin-loaded PLA nanoparticles presented results comparable with curcumin-loaded liposomes, with a few exceptions. Pre-incubation with CP-1 and CP-2 led to a reduction in MTT formation from $99.57 \pm 7.02\%$ using 0.2 mM PQ only to $79.13 \pm 8.58\%$ and $33.17 \pm 8.8\%$, respectively. Furthermore, pre-incubating with CP-2 reduced the %viability from $41.28 \pm 7.58\%$ using 0.4 mM PQ to $20.33 \pm 6.58\%$. On the other hand, the %viability increased to $67.11 \pm 8.92\%$ when pre-incubating with CP-1. Pre-incubating with both CP-1 & CP-2 led to slight inconsequential increases in the %viability after treatment with 0.6, 0.8, and 1 mM PQ. Mean \pm SD, N = 6, $p < 0.0001$, $*p < 0.05$, $**p < 0.01$, $****p < 0.0001$ compared to PQ only [Figure 10]. The increase in PQ concentration led to a gradual increase in LDH release, which was not corrected when pre-incubating with CP-1 until reaching 0.8 and 1 mM PQ. Pre-incubating with CP-2 led to complete cell death, irrespective of the PQ concentration, as shown in Figure 11. Mean \pm SD, N = 6, $p < 0.0001$, $**p < 0.01$, $***p < 0.001$, $****p < 0.0001$ compared to PQ only.

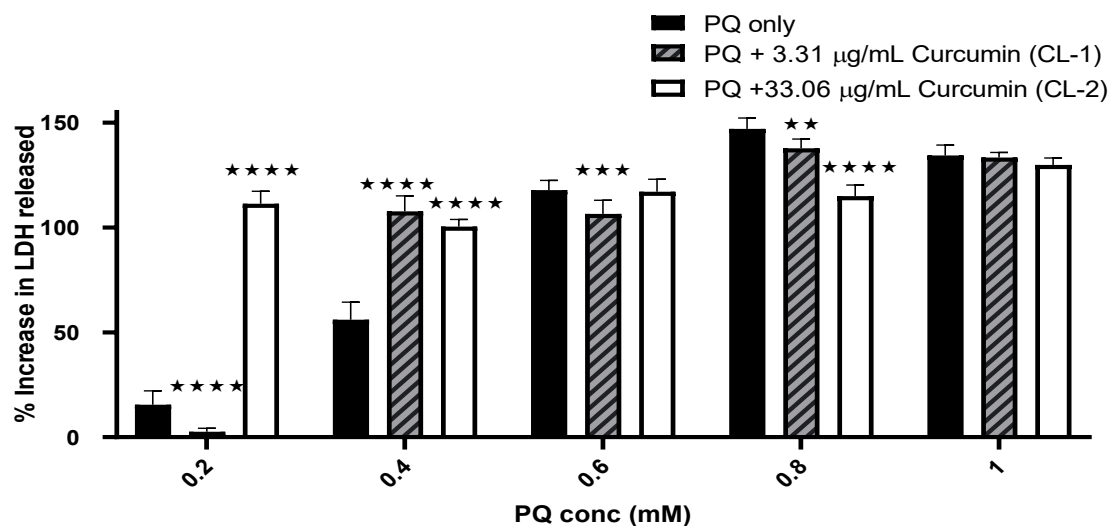


Figure 9. The effect of two different concentrations of curcumin-loaded liposomes plus PQ compared to PQ only on the %increase in LDH release from cells

Effect of pre-incubation with curcumin solution (unencapsulated form)

The pre-incubation of curcumin solution before the treatment with PQ showed comparable but less detrimental effects than its encapsulated form. As discussed previously, low doses of PQ (0.2 mM) led to a slight increase in %viability ($107.14 \pm 9.61\%$), which was further increased by pre-incubation with CS-1 to $115.11 \pm 6.03\%$ (unlike CL-1 & CP-1). Though pre-incubation with CS-2 led to a drop in the %viability ($30.34 \pm 5.38\%$), as observed with CL-2 & CP-2. Pre-incubation with CS-1 & CS-2, led to a decrease in %viability from $72.99 \pm 10.00\%$ (using 0.4 mM PQ) to $61.33 \pm 8.13\%$ & $25.17 \pm 7.29\%$; respectively, as shown when pre-incubating with CL-1 & CL-2. Though no considerable effect was noticed when pre-incubating with CS-1 after the treatment with ≥ 0.6 mM PQ, there was a minor increase in %viability when

pre-incubating with CS-2. Mean \pm SD, N = 6, $p < 0.0001$), * $p < 0.05$, **** $p < 0.0001$ compared to PQ only [Figure 12]. The results from the LDH assay showed no distinguished effect from pre-incubation with CS-1 at all PQ doses. Conversely, a variable effect was observed when pre-incubating with CS-2. At first, the %increase in LDH increased from $5.47 \pm 0.17\%$ (using 0.2 mM PQ only) to $21.8 \pm 1.57\%$ when pre-incubating with CS-2, followed by no effect on the treatment with 0.4 mM PQ. However, the protective effect of pre-incubating with CS-2 on the treatment with PQ (≥ 0.6 mM) was not noticeable. The %increase in LDH formed was reduced from $75.19 \pm 8.63\%$ (using 0.6 mM PQ) to $31.43 \pm 4.02\%$, from $84.11 \pm 6.51\%$ (using 0.8 mM PQ) to $41.17 \pm 4.05\%$, and from $112.69 \pm 8.95\%$ (using 1 mM PQ) to $30.67 \pm 2.51\%$, when pre-incubating with CS-2. Mean \pm SD, r = 6, $p < 0.0001$, * $p < 0.05$, **** $p < 0.0001$ compared to PQ only [Figure 13]. This protection was not noted with curcumin in its encapsulated forms.

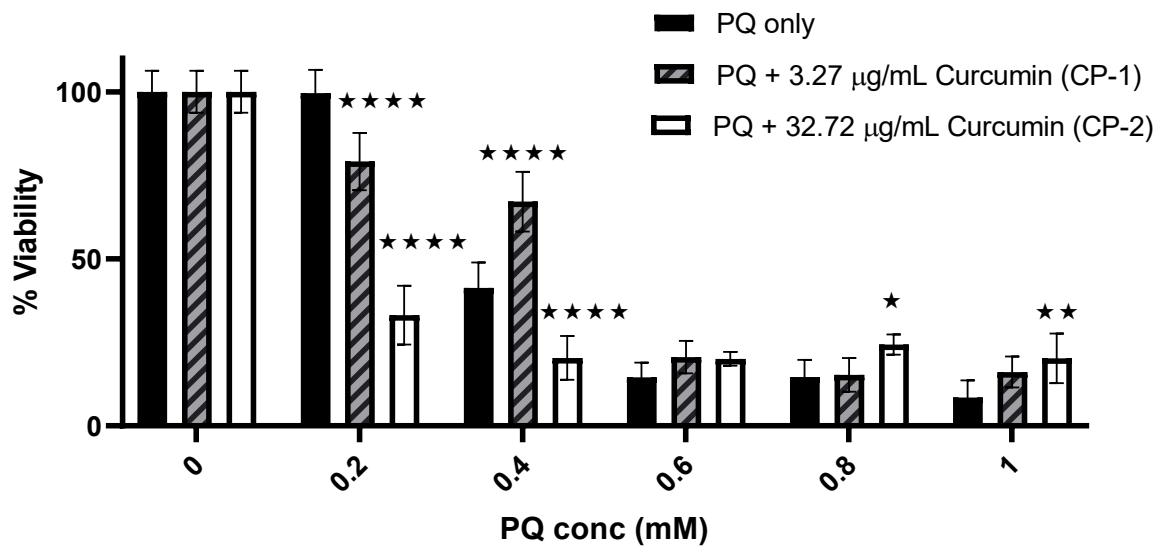


Figure 10. The effect of two different concentrations of curcumin-loaded PLA nanoparticles plus PQ compared to PQ only on %viability of cells using MTT assay

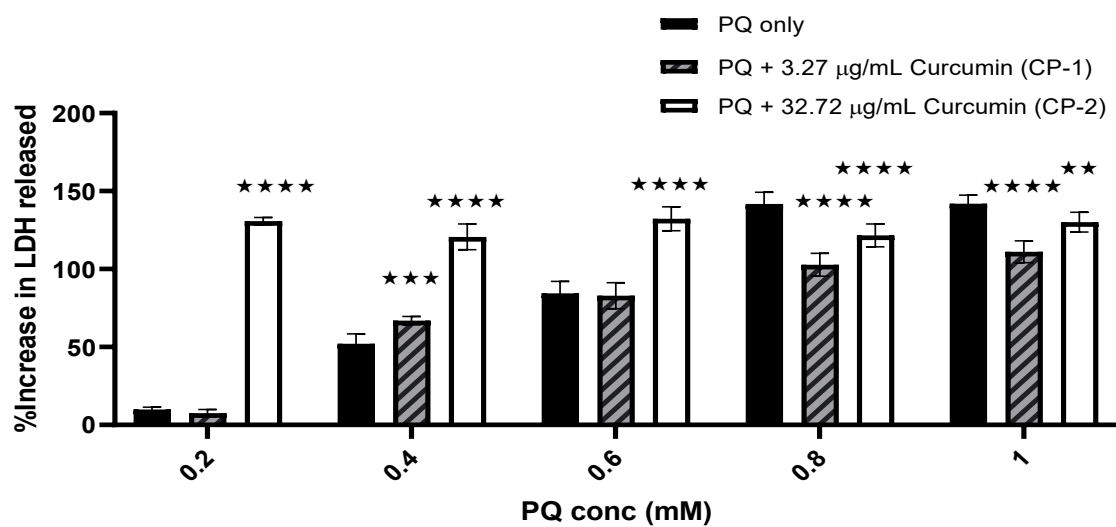


Figure 11. The effect of two different concentrations of curcumin-loaded PLA nanoparticles plus PQ compared to PQ only on the %increase in LDH release from cells

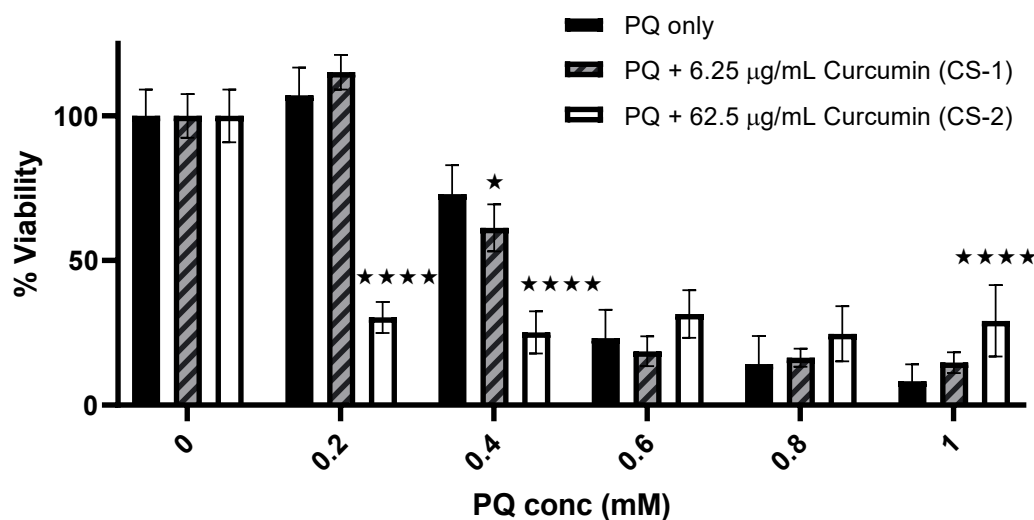


Figure 12. The effect of two different concentrations of curcumin solution plus PQ compared to PQ only on %viability of cells using the MTT assay

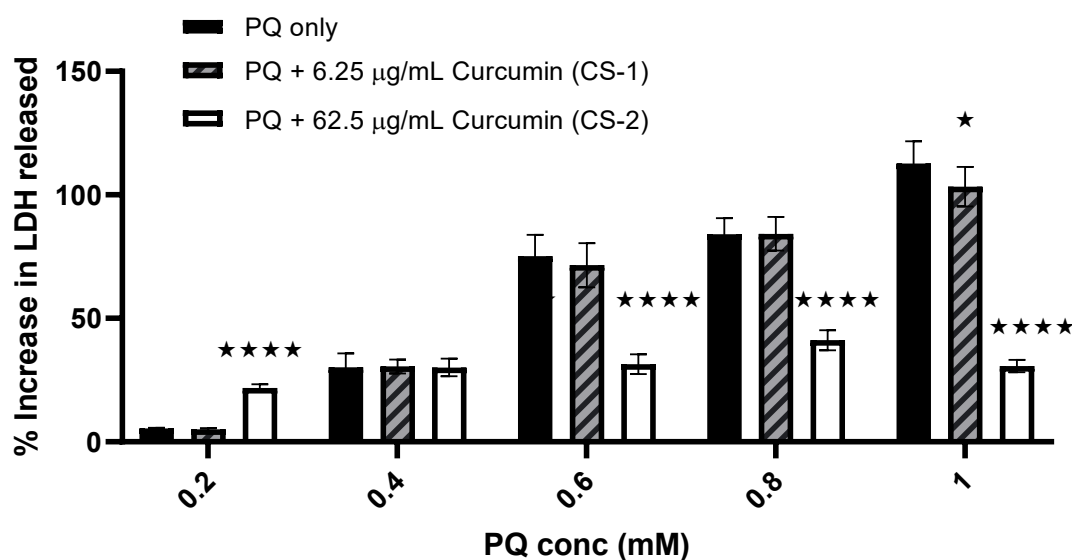


Figure 13. The effect of two different concentrations of curcumin solution plus PQ compared to PQ only on the %increase in LDH release from cells

Discussion

Curcumin is a phenolic compound that has been consumed as a traditional remedy and as a spice for centuries in many diverse countries. Research has shown its potential as an antioxidant, anti-inflammatory, anti-diabetes, anti-carcinogenic, and anti-angiogenesis compound. However, low bioavailability, poor pharmacokinetics, insolubility in water, and low stability at pH ≥ 7 are issues that reduce its potential *in vivo*. The use of nanoparticles, such as PLGA nanoparticles, has demonstrated the possible enhancement of their cellular uptake and anti-tumour activity (Punfa *et al.*, 2012). In the current study, the methods described above were used to encapsulate curcumin in both liposomes and PLA nanoparticles.

Microscopy of liposome samples indicated spherical morphology and yellow pigmentation consistent with curcumin content. The observations suggested the preparation produced a mixture of small and larger vesicles (e.g., LUV and SUV). Optical microscopy estimates were conducted using a graticule range (150–300 nm), consistent with prior thin-

film hydration-based methods that often yield multilamellar structures unless downsizing steps are applied. (Yasmin *et al.*, 2014, Degim *et al.*, 2010.) Similar images have been posted by Nguyen *et al.* (2016). They showed that curcumin-loaded liposomes made from DOPE formed liposomes in the micro-range, and when applying sonication as a downsizing technique, they formed liposomes < 100 nm in size (Nguyen *et al.*, 2016). The images from LM for liposomes, however, were not clear and do not give a clear morphology of the liposomes, due to the limitations of the instrument. It was not applicable to use SEM on liposomes due to their delicate state. Freeze-drying liposomes leads to loss of structure and formation of lumps and crystal material. Additionally, applying high negative pressure during imaging could also disrupt its structure. However, the shape of the nanoparticle in the SEM images was spherical, with a smooth surface and a variable size. It cannot be determined using only SEM whether PLA nanoparticles are nanospheres or nanocapsules. The absence of any residual drug crystals in these images indicates that no washing step was essential after the centrifugation stage. Rachmawati *et al.* (2016 and Moorkoth & Nampoothir (2014) also found that both blank and curcumin-loaded particles were smooth and spherical in their study.

In the thermal tests on PLA nanoparticles, an endothermic response was detected in all thermograms in the range 40-46 °C, including PLA standard representing the Tg of PLA. This indicates that the glass transition phase of the PLA was not influenced by the preparation process. This Tg of PLA was also described in previous studies (Buhecha *et al.*, 2019). Although the melting point of curcumin was reported in a previous work at 180 °C, with a thermal decomposition occurring at two steps, 205-441 °C, 441-630 °C (Fugita *et al.*, 2012). In the current study, however, there was only a small endothermic peak around 210 °C. The absence of the curcumin melting peak in curcumin-loaded nanoparticles has been reported previously. It was explained by the interaction of curcumin inside the nanoparticles, signifying that curcumin was in an amorphous form (Rachmawati *et al.*, 2016).

Ideally, samples would have been heated to a higher temperature, but due to the instrument limitation, the heating range was set between 25 and 250 °C. In this study, the endothermic peak around 210 °C could be due to the beginning of curcumin decomposition, as explained by Fugita *et al.*, although this peak was not observed in the work proposed by Rachmawati *et al.* (2016). During the first and second day of stability tests on liposomes, the mean particle size was comparable to all the liposomal samples formed in this study, although a slight insignificant growth was noticed on the second day. The actual size distribution curve on these first days was represented as a single sharp peak. Furthermore, the PDI was less than 0.2. These two indicators show that the particles were monodisperse. From day 3, however, a second peak was noticed in the particle size distribution graph. This has been attributed to aggregation (flocculation) or fusion (coalescence) (Yadav *et al.*, 2011). This behavior demonstrates that liposomes are physically unstable. This has also been shown in other studies of liposomes prepared from pure DPPC. For instance, results from a study on the influence of cyclodextrins on the stability of liposomes showed that both size and PDI increase upon short-term storage (7 days) of DPPC-only liposomes (Puskas & Csempesz, 2007).

This coalescence upon storage has also been stated with other neutral liposomes, such as DSPC liposomes studies but not with positively or negatively charged liposomes. The stability of charged liposomes was explained by the electrostatic repulsive forces that prevent aggregation (Katragadda *et al.*, 1999). For this reason, liposomal samples were made freshly for each subsequent test. In the MTT and LDH tests (viability and death studies), using high doses of curcumin showed a significant reduction in cell viability. This was consistent with previous reported results by Moustapha *et al.* They showed that using 25 µM (\approx 9.2 µg/mL) curcumin triggered cell death by 50% to human hepatoma-derived (Huh-7) cells. According to their study, this was equivalent to 1.25 µM (0.46 µg/mL) intracellular concentration (Moustapha *et al.*, 2015). Unpredicted and inconsistent with the literature were the results obtained using curcumin-loaded liposomes and PLA nanoparticles. The increase in the LDH release in the LDH assay was not consistent with a minimal reduction in the %viability obtained from the MTT assay or with microscopic examination. The possible clarification is the interference of the yellow color of curcumin in the LDH assay. The MTT and LDH results after pre-incubating with different curcumin formulations and giving PQ were in some way conflict-ridden. For instance, a high concentration of curcumin solution showed an enhanced harmful effect when treated with a low concentration of PQ. However, the same concentration of curcumin showed attenuation of the effect of PQ at higher concentrations. These controversial results were also observed using curcumin-loaded liposomes and PLA nanoparticles, which were, however, more detrimental than the unencapsulated form. The debatable results were also observed in other studies. For example, a study by Nikdad *et al.* showed that 100 mg/kg curcumin and 100 mg/kg nano-

curcumin ameliorated the oxidative stress induced by 5 mg/kg PQ on liver mitochondria of Wistar rats, with nano-curcumin being more potent than the free form. Here, the activity of curcumin was measured by MTT, FRAP assay, TBA assay, CAT, and SOD activity assays (Nikdad *et al.*, 2020). Another study, on the other hand, showed that 10 nM curcumin upsurges cell death (using rat mesencephalon-derived cell line) in cells treated with 0.1, 0.25, and 0.5mM PQ. The study also described that significant cell death was shown using curcumin only at doses higher than 10 μ M. (Ortiz-Ortiz *et al.*, 2009). Furthermore, a distinct study specified that whether curcumin acts as an antioxidant or pro-oxidant relies on its concentration (Banerjee *et al.*, 2008).

This study measured the hemolysis, TBA assay, potassium ion loss, and GSH concentration as markers of RBC cell viability and AAPH to induce oxidative stress. Curcumin reduced hemolysis by AAPH at an IC₅₀ of $43 \pm 5 \mu$ M but also induced hemolysis even at 50 μ M. However, this high concentration of curcumin did not cause lipid peroxidation as measured by the TBA assay. In fact, it protected the cell membrane from lipid peroxidation caused by AAPH at an IC₅₀ of $23.2 \pm 2.5 \mu$ M. Conflicting, potassium loss was augmented after treatment with all concentrations of curcumin. However, the reduction in GSH release caused by AAPH was amended using 10 μ M curcumin and further inhibited using higher doses of curcumin (Banerjee *et al.*, 2008). However, a review article by Nelson *et al.* (2017) Unfolding the properties of curcumin has described an interesting point of view in which curcumin has been classified as a pan-assay interference substance (PAINS) and an invalid metabolic panacea (IMPS), and doubts most articles describing its activity. PAINS are compounds that give false positive results mostly by interfering with the assay, and IMPS are mostly ambiguous or poor lead compounds found in natural products (Nelson *et al.*, 2017).

It should be noted that the possible interference from curcumin in the tests was not considered when performing the tests in this study. It was presumed that because curcumin was pre-incubated with the cells and washed off prior to PQ application and testing, there would be no interference. Yet, looking at the graphs from the LDH assay, mainly from curcumin-loaded liposomes and PLA nanoparticles, shows an unexpectedly high %increase in LDH release. This might be explained by interference in the absorbance readings. Encapsulating curcumin into liposomes or PLA nanoparticles augmented its solubility and could explain why readings were much higher. To resolve this possibility, the media from cells treated with the same concentrations of curcumin samples should be measured for absorbance and used as a blank or control in calculations. This can be repeated and applied in future work.

Conclusion

In this study, curcumin was successfully encapsulated into both liposomes and PLA nanoparticles and evaluated in NRK-52E cells. Physicochemical characterization confirmed the formation of curcumin-loaded systems and enabled quantification of formulation efficiency metrics, with PLA nanoparticles showing measurable drug loading and encapsulation efficiency. Thermal analysis supported retention of PLA glass transition behavior, while the absence of clear curcumin melting features in DSC thermograms was consistent with curcumin being present in a non-crystalline or molecularly dispersed state within the nanoparticle matrix. Biological evaluation revealed that curcumin can exert dose-dependent effects on NRK-52E cells, with higher concentrations reducing viability and increasing LDH release. In paraquat (PQ) oxidative stress challenge experiments, curcumin-loaded formulations did not demonstrate consistent antioxidant protection across all conditions. In several instances, encapsulated curcumin produced results that differed from those obtained with free curcumin solution, suggesting that formulation-dependent uptake and release kinetics—and potentially assay-related interference—may strongly influence observed outcomes. Overall, these findings indicate that while curcumin-loaded liposomes and PLA nanoparticles are feasible delivery systems, their biological performance in oxidative injury models is highly context-dependent. Future work should prioritize formulation-matched assay controls and additional orthogonal validation of cytotoxicity and intracellular delivery to distinguish true biological effects from readout interference.

References

1. Abe K, Matsuki N. Measurement of cellular 3-(4,5-dimethylthiazol-2-yl)-2,5-diphenyltetrazolium bromide (MTT) reduction activity and lactate dehydrogenase release using MTT. *Neurosci Res.* 2000;38(4):325-9.
2. Banerjee A, Kunwar A, Mishra B, Priyadarsini K. Concentration dependent antioxidant/pro-oxidant activity of curcumin: Studies from AAPH induced hemolysis of RBCs. *Chem Biol Interact.* 2008;174(2):134-9.



3. Buhecha M, Lansley B, Somavarapu S, Pannala S. Development and characterization of PLA nanoparticles for pulmonary drug delivery: Co-encapsulation of theophylline and budesonide, a hydrophilic and lipophilic drug. *J Drug Deliv Sci Technol.* 2019;53:101128.
4. Chen X, Sun J, Li H, Wang H, Lin Y, Hu Y, Zheng D. Curcumin-loaded nanoparticles protect against rhabdomyolysis-induced acute kidney injury. *Cell Physiol Biochem.* 2017;43:2143-54.
5. Degim Z, Agardan N, Nacar A, Yilmaz S. Investigation of liposome formulation effects on rivastigmine transport through human colonic adenocarcinoma cell line (CACO-2). *Pharmazie.* 2010;65(1):32-40.
6. Dichello G, Fukuda T, Maekawa T, Whitby R, Mikhailovsky S, Alavijeh M, Pannala A, Sarker D. Preparation of liposomes containing small gold nanoparticles using electrostatic interactions. *Eur J Pharm Sci.* 2017;105:55-63.
7. Elisha-Lambert B. The role of dietary antioxidants against oxidant-induced acute kidney injury [PhD thesis]. Brighton (UK): University of Brighton; 2017.
8. Esatbeyoglu T, Huebbe P, Ernst I, Chin D, Wagner A, Rimbach G. Curcumin—from molecule to biological function. *Angew Chem Int Ed Engl.* 2012;51(22):5308-32.
9. Fan Y, Chen H, Peng H, Haung F, Zhong J, Zhou J. Molecular mechanisms of curcumin renoprotection in experimental acute renal injury. *Front Pharmacol.* 2017;8:912.
10. Fugita R, Galico D, Guerra G, Perpetuo G, Treu-Filho O, Galhiane M, Mendes R, Bannach G. Thermal behaviour of curcumin. *Braz J Therm Anal.* 2012;1(1).
11. Garg A, Devereaux P, Hill A, Sood M, Aggarwal B, Dubois L, Hiremath S, Guzman R, Iyer V, James M, McArthur E, Moist L, Ouellet G, Parikh C, Schumann V, Sharan S, Thiessen-Philbrook H, Tobe S, Wald R, Walsh M, Weir M, Pannu N; Curcumin AAA AKI Investigators. Oral curcumin in elective abdominal aortic aneurysm repair: A multicentre randomized controlled trial. *CMAJ.* 2018;190(48):E1425.
12. Hismiogullari A, Hismiogullari S, Karaca O, Sunay F, Paksoy S, Can M, Kus I, Serek K, Yuvuz O. The protective effect of curcumin administration on carbon tetrachloride (CCl₄)-induced nephrotoxicity in rats. *Pharmacol Rep.* 2015;67(3):410-6.
13. Katragadda A, Singh M, Betageri G. Encapsulation, stability, and in vitro release characteristics of liposomal formulations of stavudine (D4T). *Drug Deliv.* 1999;6(1):31-7.
14. Kaur A, Kaur T, Singh B, Pathak, Buttar H, Singh A. Curcumin alleviates ischemia reperfusion-induced acute kidney injury through NMDA receptor antagonism in rats. *Ren Fail.* 2016;38(9):1462-7.
15. Liu F, Ni W, Zhang J, Wang G, Li F, Ren W. Administration of curcumin protects kidney tubules against renal ischemia-reperfusion injury (RIRI) by modulating nitric oxide (NO) signalling pathway. *Cell Physiol Biochem.* 2017;44:401-11.
16. Mercantepe F, Mercantepe T, Topcu A, Yilmaz A, Tumkaya A. Protective effects of amifostine, curcumin, and melatonin against cisplatin-induced acute kidney injury. *Naunyn Schmiedebergs Arch Pharmacol.* 2018;391(9):915-31.
17. Moorkoth D, Nampoothiri K. Synthesis, colloidal properties and cytotoxicity of biopolymer nanoparticles. *Appl Biochem Biotechnol.* 2014;174(6).
18. Mossmann T. Rapid colorimetric assay for cellular growth and survival: Application to proliferation and cytotoxicity assays. *J Immunol Methods.* 1983;65:55-63.
19. Moustapha A, Peretout P, Rainey N, Sureau F, Geze M, Petit J, Dewailly E, Slomianny C, Petit P. Curcumin induces crosstalk between autophagy and apoptosis mediated by calcium release from the endoplasmic reticulum, lysosomal destabilization and mitochondrial events. *Cell Death Discov.* 2015;1:15017.
20. Nabavi S, Moghaddam A, Eslami S, Nabavi M. Protective effects of curcumin against sodium fluoride-induced toxicity in rat kidneys. *Biol Trace Elem Res.* 2011;145(3):369-74.
21. Najafi H, Ashtiyani S, Sayedzadeh S, Yarijani Z, Fakhri S. Therapeutic effects of curcumin on the functional disturbances and oxidative stress induced by renal ischemia/reperfusion in rats. *Avicenna J Phytomed.* 2015;5(6):576-86.
22. Nelson K, Dahlin J, Bisson J, Graham J, Pauli G, Walters M. The essential medicinal chemistry of curcumin. *J Med Chem.* 2017;60(5):1620-37.
23. Nguyen T, Tang Q, Daun D, Dang M. Micro and nano liposome vesicles containing curcumin for a drug delivery system. *Adv Nat Sci Nanosci Nanotechnol.* 2016;7:035003.
24. Nikdad S, Ghasemi H, Khiripour N, Ranjbar A. Antioxidative effects of nano-curcumin on liver mitochondria function in paraquat-induced oxidative stress. *Res Mol Med.* 2020;8(1):37-42.
25. Ortiz-Ortiz M, Moran J, Bravosapedro J, González-Polo B, Niso-Santano M, Anantharam V, Kanthasamy A, Soler G, Fuentes J. Curcumin enhances paraquat-induced apoptosis of N27 mesencephalic cells via the generation of reactive oxygen species. *Neurotoxicology.* 2009;30(6):1008-18.
26. Priyadarsini K. The chemistry of curcumin: From extraction to therapeutic agent. *Molecules.* 2014;19:20091-112.



27. Punfa W, Yodkeeree S, Pitchakarn P, Ampasavate C, Limtrakul P. Enhancement of cellular uptake and cytotoxicity of curcumin-loaded PLGA nanoparticles by conjugation with anti-P-glycoprotein in drug resistance cancer cells. *Acta Pharmacol Sin.* 2012;33(6):823-31.
28. Puskas I, Csempesz F. Influence of cyclodextrins on the physical stability of DPPC-liposomes. *Colloids Surf B Biointerfaces.* 2007;58(2):218-24.
29. Rachmawati H, Yanda Y, Rahma A, Mase N. Curcumin-loaded PLA nanoparticles: Formulation and physical evaluation. *Sci Pharm.* 2016;84(1):191-202.
30. Rogers M, Stephenson M, Kitching A, Horowitz J, Coates P. Amelioration of renal ischaemia-reperfusion injury by liposomal delivery of curcumin to renal tubular epithelial and antigen-presenting cells. *Br J Pharmacol.* 2011;166:194-209.
31. Stanic Z. Curcumin, a compound from natural sources, a true scientific challenge - A review. *Plant Foods Hum Nutr.* 2017;72(1):1-12.
32. Tapia E, Sanchez-Lozada L, Garcia-Nino W, Garcia E, Cerecedo A, Garcia-Arroyo E. Curcumin prevents maleate-induced nephrotoxicity: Relation to hemodynamic alterations, oxidative stress, mitochondrial oxygen consumption and activity of respiratory complex I. *Free Radic Res.* 2014;48(11):1342-54.
33. Topcu-Tarladacalisir Y, Sapmaz-Metin M, Karaca T. Curcumin counteracts cisplatin-induced nephrotoxicity by preventing renal tubular cell apoptosis. *Ren Fail.* 2016;38(10):1741-8.
34. Ugur S, Ulu R, Dogukan D, Gurel A, Pembegul Y, Gozel N. The renoprotective effect of curcumin in cisplatin-induced nephrotoxicity. *Ren Fail.* 2014;37(2):332-6.
35. Yadav R, Kumar D, Kumari A, Yadav S. Encapsulation of catechin and epicatechin on BSA NPS improved their stability and antioxidant potential. *EXCLI J.* 2014;13:331-46.
36. Yasmin H, Murugesan R, Girigoswami A. Gene expression profile induced by liposomal nanoformulation of anticancer agents: Insight into cell death mechanism. *Adv Sci Eng Med.* 2014;6(2):159-65.